Thermal Convection for Large Prandtl Numbers

Siegfried Grossmann[1] and Detlef Lohse[2]

[1]*Department of Physics, University of Marburg, Renthof 6, D-35032 Marburg, Germany*
[2]*Department of Applied Physics and J. M. Burgers Centre for Fluid Dynamics, University of Twente, 7500 AE Enschede, The Netherlands*

(Received 26 July 2000)

The Rayleigh-Bénard theory by Grossmann and Lohse [J. Fluid Mech. **407**, 27 (2000)] is extended towards very large Prandtl numbers Pr. The Nusselt number Nu is found here to be independent of Pr. However, for fixed Rayleigh numbers Ra a maximum in the Nu(Pr) dependence is predicted. We moreover offer the full functional dependences of Nu(Ra,Pr) and Re(Ra,Pr) within this extended theory, rather than only give the limiting power laws as done in J. Fluid. Mech. **407**, 27 (2000). This enables us to more realistically describe the *transitions* between the various scaling regimes.

DOI: 10.1103/PhysRevLett.86.3316 PACS numbers: 47.27.–i, 47.27.Te

In thermal convection, the control parameters are the Rayleigh number Ra and the Prandtl number Pr. The system responds with the Nusselt number Nu (the dimensionless heat flux) and the Reynolds number Re (the dimensionless large scale velocity U). The key question is to understand the dependences Nu(Ra,Pr) and Re(Ra,Pr). In experiments, traditionally the Prandtl number was more or less kept fixed [1–3]. However, the recent experiments in the vicinity of the critical point of helium gas [4,5] and of SF_6 [6] or with various alcohols [7,8] allow one to vary both Ra and Pr and thus to explore a larger domain of the Ra-Pr parameter space of Rayleigh-Bénard (RB) convection, in particular that for $\mathrm{Pr} \gg 1$. The experiments of Ahlers and co-workers [7,8] suggest that for $2 \leq \mathrm{Pr} \leq 34$ the Nusselt number only weakly decreases with increasing Pr and perhaps even saturates [9]. The same (at fixed $\mathrm{Ra} = 6 \times 10^5$) is found in the numerical simulations [10,11].

The large Pr regime of the latest experiments has not been covered by the recent theory on thermal convection by Grossmann and Lohse (GL, [12]), which otherwise well describes various measurements. In particular, it explains the low Pr measurements of Cioni *et al.* [3] ($\mathrm{Pr} = 0.025$), the low Pr numerics which reveal $\mathrm{Nu} \sim \mathrm{Pr}^{0.14}$ for fixed Ra [10,11], and the above mentioned experiments by Niemela *et al.* [5] and Xu *et al.* [7].

One main result of the present work is that Nu is found to be independent of Pr in the large Pr regime. We in addition present the complete functional dependences Nu(Ra,Pr) and Re(Ra,Pr) within the GL approach, rather than only giving the limiting power laws and superpositions of those as was done in [12]. This enables us to more realistically model the *transitions* between the scaling regimes of [12].

Approach.—To make this paper self-contained we very briefly recapitulate the key idea of the GL theory, which is to decompose the energy dissipation rate ϵ_u and the thermal dissipation rate ϵ_θ into their boundary layer (BL) and bulk contributions,

$$\epsilon_u = \epsilon_{u,\mathrm{BL}} + \epsilon_{u,\mathrm{bulk}}, \tag{1}$$

$$\epsilon_\theta = \epsilon_{\theta,\mathrm{BL}} + \epsilon_{\theta,\mathrm{bulk}}. \tag{2}$$

For the left-hand sides the exact relations $\epsilon_u = \frac{\nu^3}{L^4}(\mathrm{Nu} - 1)\,\mathrm{Ra}\,\mathrm{Pr}^{-2}$ and $\epsilon_\theta = \kappa\frac{\Delta^2}{L^2}\,\mathrm{Nu}$ are used, where ν is the kinematic viscosity, κ the thermal diffusivity, L the height of the cell, and Δ the temperature differences between bottom and top plates. The local dissipation rates in the BL and in the bulk [right-hand sides of Eqs. (1) and (2)] are modeled as the corresponding energy input rates, i.e., in terms of U, Δ, L, and the widths λ_u and λ_θ of the kinetic and thermal boundary layers, respectively. For the thickness of the thermal BL we assume $\lambda_\theta = L/(2\,\mathrm{Nu})$ and for that of the kinetic one $\lambda_u = L/(4\sqrt{\mathrm{Re}})$ as it holds in Blasius type layers [13]; as for the prefactor $1/4$ cf. [12], Sec. 3.4. For very large Ra the laminar BL will become turbulent and λ_u will show a stronger Re dependence. Note that whereas the thermal BLs build up only at the top and bottom wall, the kinetic BL occurs at *all* walls of the cell and therefore the contribution of $\epsilon_{u,\mathrm{BL}}$ to ϵ_u is larger than a simple minded argument would suggest. The two Eqs. (1) and (2) then allow one to calculate the two dependent variables Nu and Re as functions of the two independent ones Ra and Pr.

Input rate modeling.—The modeling of the dissipation rates on the rhs of Eqs. (1) and (2) is guided by the Boussinesq equations. Depending on whether the BL or the bulk contributions are dominant, one gets different expressions on the rhs of Eqs. (1) and (2) and thus different relations for Nu, Re vs Ra, Pr, defining different main regimes; see Ref. [12] and Fig. 1.

The rhs thermal dissipation rates depend on whether the kinetic BL of thickness λ_u is within the thermal BL of thickness λ_θ ($\lambda_u < \lambda_\theta$, small Pr) or vice versa ($\lambda_u > \lambda_\theta$, large Pr). The line $\lambda_u = \lambda_\theta$, corresponding to $\mathrm{Nu} = 2\sqrt{\mathrm{Re}}$, splits the phase diagram into a lower (small Pr) and an upper (large Pr) part, which we label by "l" and "u".

We first consider $\lambda_u < \lambda_\theta$ (i.e., small Pr, regime "l"). Then (see [12])

 0031-9007/01/86(15)/3316(4)$15.00

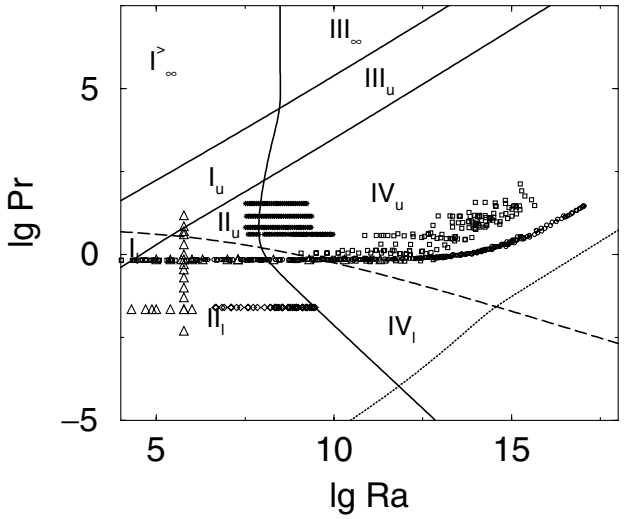

FIG. 1. Phase diagram in the Ra-Pr plane: The upper solid line means $\mathrm{Re} = \mathrm{Re}_c$ (≈ 0.28), the lower nearly parallel solid line $\epsilon_{u,\mathrm{BL}} = \epsilon_{u,\mathrm{bulk}}$, the curved solid line is $\epsilon_{\theta,\mathrm{BL}} = \epsilon_{\theta,\mathrm{bulk}}$, and the long-dashed line is the line $\lambda_u = \lambda_\theta$. The thin dotted line denotes where the laminar kinetic BL becomes turbulent. As extensively discussed in Ref. [12], the exact onset of this instability strongly depends on the prefactors used when calculating this type of phase diagram. Data points where Nu has been measured or numerically calculated have been included; squares: Chavanne *et al.* [4]; diamonds: Cioni *et al.* [3]; circles: Niemela *et al.* [5]; stars: Xu *et al.* [7,8]; triangles: Verzicco and Camussi (numerical simulations) [10].

$$\epsilon_{u,\mathrm{bulk}} \sim \frac{U^3}{L} \sim \frac{\nu^3}{L^4}\,\mathrm{Re}^3, \tag{3}$$

$$\epsilon_{u,\mathrm{BL}} \sim \nu\,\frac{U^2}{\lambda_u^2}\frac{\lambda_u}{L} \sim \frac{\nu^3}{L^4}\,\mathrm{Re}^{5/2}, \tag{4}$$

$$\epsilon_{\theta,\mathrm{bulk}} \sim \frac{U\Delta^2}{L} \sim \kappa\,\frac{\Delta^2}{L^2}\,\mathrm{Pr}\,\mathrm{Re}\,, \tag{5}$$

$$\epsilon_{\theta,\mathrm{BL}} \sim \kappa\,\frac{\Delta^2}{L^2}\,(\mathrm{Re}\,\mathrm{Pr})^{1/2}. \tag{6}$$

The last expression is concluded [2,12] from the heat transfer equation $u_x\partial_x\theta + u_z\partial_z\theta = \kappa\partial_z^2\theta$, which implies $U/L \sim \kappa/\lambda_\theta^2$ giving $\mathrm{Re}^{1/2}\,\mathrm{Pr}^{1/2} \sim \mathrm{Nu}$.

If now larger Pr are considered, the kinetic boundary will eventually exceed the thermal one, $\lambda_u > \lambda_\theta$, upper range "$u$". The relevant velocity at the edge between the thermal BL and the thermal bulk now is less than U, namely about $U\lambda_\theta/\lambda_u$. To describe the transition from λ_u being smaller to being larger than λ_θ we introduce the function $f(x) = (1 + x^n)^{-1/n}$ of the variable $x_\theta = \lambda_u/\lambda_\theta = \mathrm{Nu}/2\sqrt{\mathrm{Re}}$, f being 1 in the lower range "l" (small Pr) and $1/x_\theta$ in "u" (large Pr), respectively. The relevant velocity then is $Uf(x_\theta)$. We take $n = 4$ to characterize the sharpness of the transition.

This generalizes (5),(6) to

$$\epsilon_{\theta,\mathrm{bulk}} \sim \kappa\,\frac{\Delta^2}{L^2}\,\mathrm{Pr}\,\mathrm{Re} f(\mathrm{Nu}/2\sqrt{\mathrm{Re}}\,), \tag{7}$$

$$\epsilon_{\theta,\mathrm{BK}} \sim \kappa\,\frac{\Delta^2}{L^2}\sqrt{\mathrm{Pr}\,\mathrm{Re} f(\mathrm{Nu}/2\sqrt{\mathrm{Re}}\,)}, \tag{8}$$

while $\epsilon_{u,\mathrm{bulk}}$ and $\epsilon_{u,\mathrm{BL}}$ are still given by (3),(4). Introducing (3),(4),(7),(8) into (1),(2) leads to the Ra,Pr dependences of Nu,Re in the upper regime "u". The pure power laws Nu(Ra,Pr) and Re(Ra,Pr) in both the *lower* "l" ($\lambda_u < \lambda_\theta$, small Pr) and the *upper* "u" ($\lambda_u > \lambda_\theta$, large Pr) regimes are summarized in Table I.

Very large Pr regime.—We now extend the theory to very large Prandtl numbers. As long as $\mathrm{Ra} > \mathrm{Ra}_c = 1708$ there still is wind, even for very large Pr, as Ra_c is independent of Pr. However, this large scale wind Re slows down with increasing Pr and eventually becomes laminar throughout the cell. λ_u can no longer continue to increase according to $\lambda_u = L/(4\,\mathrm{Re}^{1/2})$ with decreasing Re, but will saturate to a constant value of order L. We call the corresponding Reynolds number Re_c and $\lambda_u = L/(4\sqrt{\mathrm{Re}_c})$ in this very large Pr regime. To model the smooth transition to the very large Pr regime beyond the line $\mathrm{Re} = \mathrm{Re}_c$, i.e., if $\lambda_u(\mathrm{Re}) = L/4\sqrt{\mathrm{Re}}$ approaches $\lambda_u(\mathrm{Re}_c)$, we use the crossover function $g(x) = x(1 + x^n)^{-1/n}$ of the crossover variable $x_L = \lambda_u(\mathrm{Re})/\lambda_u(\mathrm{Re}_c) = \sqrt{\mathrm{Re}_c/\mathrm{Re}}$, and again $n = 4$. The function g increases linearly, $g(x_L) = x_L$, below the transition (x_L small) and is 1 in the very large Pr regime with $\mathrm{Re} \le \mathrm{Re}_c$. In the above modeling for the local dissipation rates we have to replace each λ_u by $g(x_L)\lambda_u(\mathrm{Re}_c)$.

The resulting formulas, given momentarily, will lead, depending on Ra, to three new regimes, valid for very large Pr, denoted as $\mathrm{I}_\infty^<$, $\mathrm{I}_\infty^>$, and III_∞; see Fig. 1 and Table I.

While Eq. (3) for $\epsilon_{u,\mathrm{bulk}}$ is assumed to still hold in the very large Pr range (where $\epsilon_{u,\mathrm{bulk}}$ hardly contributes to ϵ_u due to the large extension of the kinetic BLs), Eqs. (4)–(6) must be generalized. First generalize (4) for $\epsilon_{u,\mathrm{BL}}$,

$$\epsilon_{u,\mathrm{BL}} \sim \nu\,\frac{U^2}{g(x_L)L^2} \sim \frac{\nu^3}{L^4}\,\frac{\mathrm{Re}^2}{g(\sqrt{\mathrm{Re}_c/\mathrm{Re}})}. \tag{9}$$

Next $\epsilon_{\theta,\mathrm{bulk}}$: The wind velocity U in (5), which sets the time scale of the stirring, has already been generalized to $Uf(\lambda_u/\lambda_\theta)$. This equals U itself in the "l" and $U\lambda_\theta/\lambda_u$ in the "u" regimes. Now, in addition, the explicit λ_u is to be replaced by $g(x_L)\lambda_u(\mathrm{Re}_c)$, i.e.,

$$\epsilon_{\theta,\mathrm{bulk}} \sim \kappa\,\frac{\Delta^2}{L^2}\,\mathrm{Pr}\,\mathrm{Re} f\Big[\frac{\mathrm{Nu}}{2\sqrt{\mathrm{Re}_c}}\,g\Big(\sqrt{\frac{\mathrm{Re}_c}{\mathrm{Re}}}\Big)\Big]. \tag{10}$$

Equation (10) simplifies for large enough Ra (therefore large f argument) and very large Pr (thus large g argument) to $\epsilon_{\theta,\mathrm{bulk}} \sim \kappa\frac{\Delta^2}{L^2}\frac{\mathrm{Pr}\,\mathrm{Re}}{\mathrm{Nu}}$. Inserting (9) and (10) into the rhs of (1) and (2) leads to the new power laws describing the heat flux and the wind velocity in the regime III_∞ beyond III_u; cf. Fig. 1,

$$\mathrm{Nu} \sim \mathrm{Ra}^{1/3}\,\mathrm{Pr}^0, \qquad \mathrm{Re} \sim \mathrm{Ra}^{2/3}\,\mathrm{Pr}^{-1}. \tag{11}$$

Finally, $\epsilon_{\theta,\mathrm{BL}}$: In the thermal boundary layer range beyond I_l, relevant for medium Ra, Eq. (6) stays valid, because its derivation did not involve λ_u and also $f = 1$. The

TABLE I. The pure power laws for Nu and Re. The prefactors are based on the c_i's given after Eq. (14).

Regime	Dominance of	BLs	Nu	Re
I_l	$\epsilon_{u,\mathrm{BL}}, \epsilon_{\theta,\mathrm{BL}}$	$\lambda_u < \lambda_\theta$	$0.22\,\mathrm{Ra}^{1/4}\,\mathrm{Pr}^{1/8}$	$0.063\,\mathrm{Ra}^{1/2}\,\mathrm{Pr}^{-3/4}$
I_u		$\lambda_u > \lambda_\theta$	$0.31\,\mathrm{Ra}^{1/4}\,\mathrm{Pr}^{-1/12}$	$0.073\,\mathrm{Ra}^{1/2}\,\mathrm{Pr}^{-5/6}$
$\mathrm{I}_\infty^<$		$\lambda_u = L/(4\sqrt{\mathrm{Re}_c}) > \lambda_\theta$	$0.17\,\mathrm{Ra}^{1/3}$	$0.038\,\mathrm{Ra}^{2/3}\,\mathrm{Pr}^{-1}$
$\mathrm{I}_\infty^>$		$\lambda_u = L/(4\sqrt{\mathrm{Re}_c}) > \lambda_\theta$	$0.35\,\mathrm{Ra}^{1/5}$	$0.054\,\mathrm{Ra}^{3/5}\,\mathrm{Pr}^{-1}$
II_l	$\epsilon_{u,\mathrm{bulk}}, \epsilon_{\theta,\mathrm{BL}}$	$\lambda_u < \lambda_\theta$	$0.37\,\mathrm{Ra}^{1/5}\,\mathrm{Pr}^{1/5}$	$0.17\,\mathrm{Ra}^{2/5}\,\mathrm{Pr}^{-3/5}$
II_u		$\lambda_u > \lambda_\theta$	$0.51\,\mathrm{Ra}^{1/5}$	$0.19\,\mathrm{Ra}^{2/5}\,\mathrm{Pr}^{-2/3}$
III_u	$\epsilon_{u,\mathrm{BL}}, \epsilon_{\theta,\mathrm{bulk}}$	$\lambda_u > \lambda_\theta$	$0.018\,\mathrm{Ra}^{3/7}\,\mathrm{Pr}^{-1/7}$	$0.023\,\mathrm{Ra}^{4/7}\,\mathrm{Pr}^{-6/7}$
III_∞		$\lambda_u = L/(4\sqrt{\mathrm{Re}_c}) > \lambda_\theta$	$0.027\,\mathrm{Ra}^{1/3}$	$0.015\,\mathrm{Ra}^{2/3}\,\mathrm{Pr}^{-1}$
IV_l	$\epsilon_{u,\mathrm{bulk}}, \epsilon_{\theta,\mathrm{bulk}}$	$\lambda_u < \lambda_\theta$	$0.0012\,\mathrm{Ra}^{1/2}\,\mathrm{Pr}^{1/2}$	$0.025\,\mathrm{Ra}^{1/2}\,\mathrm{Pr}^{-1/2}$
IV_u		$\lambda_u > \lambda_\theta$	$0.050\,\mathrm{Ra}^{1/3}$	$0.088\,\mathrm{Ra}^{4/9}\,\mathrm{Pr}^{-2/3}$

range $\mathrm{I}_\infty^<$ has to be described by Eqs. (1),(2),(9) (with $g = 1$), and (6), resulting in the same power laws as in regime III_∞, i.e., Eqs. (11). For Pr values above regime I_u Eq. (6) no longer holds. It originated from the heat transport equation. There we now have to use $Uf(x_\theta)$ instead of merely U. The balance from the heat transfer equation then reads $Uf(x_\theta)/L \sim \kappa/\lambda_\theta^2$. In the f argument $x_\theta = \lambda_u/\lambda_\theta$, the kinetic BL width λ_u and therefore the crossover function g appears, leading to $\mathrm{Pr}\,\mathrm{Re} f[\frac{\mathrm{Nu}}{2\sqrt{\mathrm{Re}_c}} g(\sqrt{\frac{\mathrm{Re}_c}{\mathrm{Re}}})] \sim \mathrm{Nu}^2$. For very large Pr [where $g(x_L) = 1$] above I_u [where $f(x_\theta) = x_\theta^{-1}$] one obtains the relation $(\mathrm{Re}\,\mathrm{Pr})^{1/3} \sim \mathrm{Nu}$, valid in $\mathrm{I}_\infty^>$. Together with (1), (2), and (9) one derives the new scaling laws in the interior of $\mathrm{I}_\infty^>$,

$$\mathrm{Nu} \sim \mathrm{Ra}^{1/5}\,\mathrm{Pr}^0, \qquad \mathrm{Re} \sim \mathrm{Ra}^{3/5}\,\mathrm{Pr}^{-1}. \tag{12}$$

The scaling behavior $\mathrm{Nu} \sim \mathrm{Ra}^{1/5}$ has earlier been suggested by Roberts [14]. Note that in all three very large Pr regimes Nu does not depend on Pr. Furthermore, the upper bound $\mathrm{Nu} \le \mathrm{const}\,\mathrm{Ra}^{1/3}(1 + \log \mathrm{Ra})^{2/3}$, holding in the limit $\mathrm{Pr} \to \infty$, is strictly fulfilled [15].

Nu *and* Re *in the whole parameter plane.*—Plugging now the generalized expressions for the local dissipation rates into the balance Eqs. (1) and (2) finally results in

$$\mathrm{Nu}\,\mathrm{Ra}\,\mathrm{Pr}^{-2} = c_1 \frac{\mathrm{Re}^2}{g(\sqrt{\mathrm{Re}_c/\mathrm{Re}})} + c_2\,\mathrm{Re}^3, \tag{13}$$

$$\mathrm{Nu} = c_3\,\mathrm{Re}^{1/2}\,\mathrm{Pr}^{1/2}\left\{f\left[\frac{\mathrm{Nu}}{2\sqrt{\mathrm{Re}_c}}\, g\left(\sqrt{\frac{\mathrm{Re}_c}{\mathrm{Re}}}\right)\right]\right\}^{1/2} + c_4\,\mathrm{Pr}\,\mathrm{Re} f\left[\frac{\mathrm{Nu}}{2\sqrt{\mathrm{Re}_c}}\, g\left(\sqrt{\frac{\mathrm{Re}_c}{\mathrm{Re}}}\right)\right]. \tag{14}$$

Here we have added the dimensionless prefactors where appropriate to complete the modeling of the dissipation rates. We have adopted them by a nonlinear fit with the Levenberg-Marquardt method [16] to 151 experimental data points Nu(Ra,Pr) obtained by Ahlers [8]; see inset of Fig. 2b for the quality of the fit. The result for aspect ratio $\Gamma = 1$ is $c_1 = 120$, $c_2 = 74$, $c_3 = 0.89$, $c_4 = 0.048$, and $\mathrm{Re}_c = 0.28$, and all plots in this paper are based on these numbers. Note that the c_i and Re_c may depend on the aspect ratio and are not universal.

The set of Eqs. (13) and (14) is the second main result of this paper. It allows one to calculate Nu(Ra,Pr) and Re(Ra,Pr) in the whole Ra-Pr parameter space, including all crossovers from any regime to any neighboring one.

All limiting, pure scaling regimes which can be derived from Eqs. (13) and (14) are listed in Table I. The corresponding phase diagram is shown in Fig. 1, completing that of [12] towards very large Pr. Though in the phase diagram we have drawn lines to indicate transitions between the regimes, we note that the crossovers are nothing at all but sharp. All transitions are smeared out of broad ranges. This holds the more, the more similar the scaling exponents of the neighboring regimes are.

Discussion of Nu(Pr) *and* Nu(Ra).—The functions Nu(Pr) (for fixed values of Ra) and $\mathrm{Nu}(\mathrm{Ra})/\mathrm{Ra}^{1/4}$ (for fixed values of Pr) resulting from Eqs. (13) and (14) are shown in Fig. 2. Nu saturates with increasing Pr. For moderate $\mathrm{Ra} = 10^6 - 10^8$ a maximum in Nu(Pr), resulting from the Nu decrease in regimes I_u and III_u, can be seen. It broadens to a plateau for larger Ra, due to the lacking Pr dependence of Nu in regime IV_u. The decrease in regime III_u from the plateau to the large Pr saturation regime is shifted to larger Pr with increasing Ra, as suggested by Fig. 1.

Figure 2b highlights the effects of having finite transition widths. For example, in regime II_l with $\mathrm{Nu} \sim \mathrm{Ra}^{1/5}$ (for fixed Pr) the corresponding scaling exponent $1/5 - 1/4 = -1/20$ becomes observable only for very small $\mathrm{Pr} \approx 10^{-3}$–$10^{-4}$. At $\mathrm{Pr} = 10^{-1}$ the roughly four decades of regime II_l (see Fig. 1) between regime I_l and IV_l, which both have a stronger Ra dependence of Nu, are not sufficient to reveal the scaling exponent. And at $\mathrm{Pr} = 10^0$ the roughly 2.5 decades of regime II_l are *nowhere* sufficient to lead to a local scaling exponent $d\lg\mathrm{Nu}/d\lg\mathrm{Ra}$ smaller than $1/4$.

Similarly, for $\mathrm{Pr} = 1$ only for very large $\mathrm{Ra} \gtrsim 10^{14}$ pure scaling $\mathrm{Nu} \sim \mathrm{Ra}^{1/3}$ is revealed. For smaller Ra regimes I_u and I_l with $\mathrm{Nu} \sim \mathrm{Ra}^{1/4}$ and II_u with $\mathrm{Nu} \sim \mathrm{Ra}^{1/5}$ strongly contribute, resulting in an effective local scaling exponent (increasing with Ra) in the range between 0.28 ("2/7") and 0.31, just as observed in experiment [1,2,4,5].

Comparison to more experiments.—In experiment, it is hard to vary either Ra or Pr over many decades *and* at

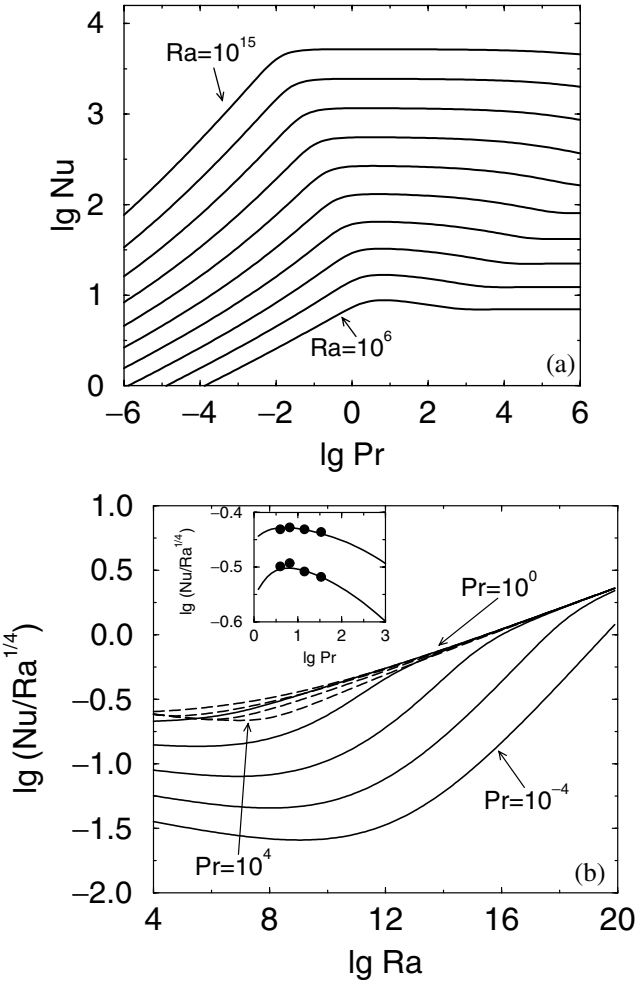

FIG. 2. (a) Nu as a function of Pr according to theory for $\mathrm{Ra} = 10^6, \mathrm{Ra} = 10^7, \ldots$ to $\mathrm{Ra} = 10^{15}$, bottom to top. (b) $\mathrm{Nu}/\mathrm{Ra}^{1/4}$ vs Ra for $\mathrm{Pr} = 10^{-4}, \ldots, \mathrm{Pr} = 10^0$ (solid lines, bottom to top) and for $\mathrm{Pr} = 10^1$, $\mathrm{Pr} = 10^2$, $\mathrm{Pr} = 10^3$, and $\mathrm{Pr} = 10^4$ (dashed lines, top to bottom). The inset shows how well the data of Ref. [8] can be fitted within this theory. $\mathrm{Ra} = 10^{9.25}$ and $\mathrm{Ra} = 10^{7.25}$ for the upper and lower curve, respectively.

the same time to keep the other variable fixed. So most measurements are done along *curved* lines in the phase space Fig. 1, mixing the Ra and Pr dependences. Now Eqs. (13) and (14) allow one to calculate Nu and Re along such a curve Pr(Ra). The present theory suggests that inspite of the different Pr numbers the Nusselt number in the Chavanne *et al.* experiment [4] should be nearly indistinguishable (due to the lacking Pr dependence of Nu in regime IV_u) to that in the Niemela *et al.* experiment [5], in contrast to what is found; see Fig. 3. Possibly, different temperature boundary conditions have been applied in the two experiments.

This research work was prompted by the experiments of G. Ahlers [8], presented to us at the ITP-Workshop in Santa Barbara in March 2000. We thank him for sharing his results with us prior to publication and for performing the side wall corrections. We also thank him and K. R. Sreenivasan for continuous discussions.

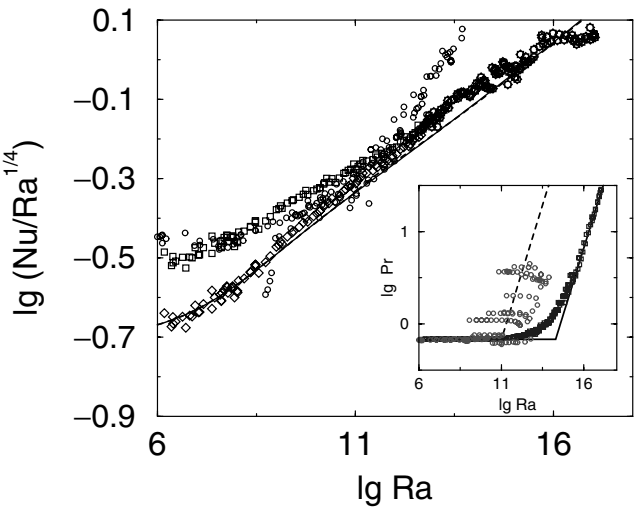

FIG. 3. $\mathrm{Nu}[\mathrm{Ra}, \mathrm{Pr}(\mathrm{Ra})]/\mathrm{Ra}^{1/4}$ along the curve Pr(Ra) (shown as boxes in the inset) given by the experimental restrictions of in the Niemela *et al.* experiment [5]. The diamonds show the side-wall-corrected (following Ref. [17]) data by Niemela *et al.,* the solid line shows the result of the present theory (whose parameters had been adopted to data [8] in a *different* parameter regime; see text). The boxes show the Niemela *et al.* data *without* sidewall corrections, and the circles show the data from the Chavanne *et al.* experiment [4] (also without sidewall corrections), which were taken along the dashed line in the inset. The Nusselt number along that line is practically indistinguishable from that one along the solid line.

[1] B. Castaing *et al.,* J. Fluid Mech. **204**, 1 (1989).
[2] E. D. Siggia, Annu. Rev. Fluid Mech. **26**, 137 (1994).
[3] S. Cioni, S. Ciliberto, and J. Sommeria, J. Fluid Mech. **335**, 111 (1997).
[4] X. Chavanne *et al.,* Phys. Rev. Lett. **79**, 3648 (1997).
[5] J. Niemela, L. Skrebek, K. R. Sreenivasan, and R. Donelly, Nature (London) **404**, 837 (2000).
[6] S. Ashkenazi and V. Steinberg, Phys. Rev. Lett. **83**, 3641 (1999).
[7] X. Xu, K. M. S. Bajaj, and G. Ahlers, Phys. Rev. Lett. **84**, 4357 (2000).
[8] G. Ahlers and X. Xu, following Letter, Phys. Rev. Lett. **86**, 3320 (2001).
[9] The experiments reported in [6] suggest a stronger decreasing Nusselt number with increasing Pr, namely $\mathrm{Nu} = 0.22\,\mathrm{Ra}^{0.3\pm0.03}\,\mathrm{Pr}^{-0.2\pm0.04}$ in $10^9 \leq \mathrm{Ra} \leq 10^{14}$ and $1 \leq \mathrm{Pr} \leq 93$.
[10] R. Verzicco and R. Camussi, J. Fluid Mech. **383**, 55 (1999).
[11] R. Kerr and J. Herring, J. Fluid Mech. **419**, 325 (2000).
[12] S. Grossmann and D. Lohse, J. Fluid Mech. **407**, 27 (2000).
[13] L. D. Landau and E. M. Lifshitz, *Fluid Mechanics* (Pergamon Press, Oxford, 1987).
[14] G. O. Roberts, Geophys. Astrophys. Fluid Dyn. **12**, 235 (1979).
[15] P. Constantin and C. Doering, J. Stat. Phys. **94**, 159 (1999).
[16] W. Press *et al., Numerical Recipes* (Cambridge University Press, Cambridge, 1986).
[17] G. Ahlers, Phys. Rev. E **63**, 015303 (2000).